

Coercivity enhancement above the Néel temperature of an antiferromagnet/ferromagnet bilayer

C. Leighton

Department of Chemical Engineering and Materials Science, University of Minnesota, Minnesota 55455

H. Suhl

Department of Physics, 0319, University of California, San Diego, La Jolla, California 92093-0319

Michael J. Pechan and R. Compton

Department of Physics, Miami University, Oxford, Ohio 45056

J. Nogués

Departament de Física, Universitat Autònoma de Barcelona, 08193 Bellaterra, Spain

Ivan K. Schuller

Department of Physics, 0319, University of California, San Diego, La Jolla, California 92093-0319

(Received 15 February 2002; accepted for publication 9 May 2002)

Single-crystal thin films of the antiferromagnet FeF_2 have been used to exchange bias overlayers of Fe. An unexpected coercivity enhancement is observed at temperatures above the Néel temperature of the FeF_2 . This coercivity reaches a peak value of over 600 Oe close to the Néel temperature and persists to above 300 K. The coercivity is correlated with the growth of an anisotropy in the ferromagnet, the increase of the antiferromagnetic susceptibility and the increase of the ferromagnetic resonance linewidth. We argue that the growth of spin fluctuations in the antiferromagnet leads to an enhanced ferromagnetic anisotropy, and therefore coercivity, above the Néel temperature. © 2002 American Institute of Physics. [DOI: 10.1063/1.1491277]

I. INTRODUCTION

Exchange anisotropy at the interface between antiferromagnets (AF) and ferromagnets (F) is a long-standing problem in materials physics.¹ The interest is due to the fact that it is a phenomenon that has escaped full explanation for 45 years² as well as being of great importance for applications.^{1,3} Although the most obvious manifestation of exchange-induced anisotropy is the exchange bias, H_E (the shift along the field axis of the hysteresis loop), it is also accompanied by an increase in the loop width, H_C .^{1,4-10} This coercivity enhancement has been the topic of many recent investigations since the realization that it is intimately related to the exchange anisotropy, displays intriguing correlations with H_E , and could contain important information on the microscopic origin of the unidirectional anisotropy.⁷ Experimentally, the H_C enhancement has been studied in several materials systems as a function of temperature,^{4,7-10,11} interface disorder,⁷ and cooling field,⁷ while several models have been advanced. These include pinning of domain walls in the F layer by perpendicular AF domains,^{4,5,7,8} irreversible changes in AF spin structure on field cycling,¹⁰ higher-order anisotropies,⁹ interfacial frustration,⁷ and uniaxial anisotropy induced by perpendicular coupling.⁶ The mechanisms of magnetization reversal in AF/F bilayers (which have recently been investigated in detail^{12,13}) are related, and are of similar significance.

In this article, we have investigated the H_C enhancement effect in a regime that is not readily accessible; untwinned single-crystal thin-film AF layers. While many studies have dealt with polycrystalline thin-film bilayers or F thin films on

single-crystal AFs,^{1,14} in this case we directly probe single-crystal *thin-film* AFs. Note that while previous papers on fluoride AF layers have dealt with twinned quasiepitaxial layers,^{7,13,15} here we deal with a completely monodomain AF systems. In this model system, we observe behavior below T_N (the AF Néel temperature), which is dominated by perpendicular coupling,^{6,14,16,17} while above T_N we observe a strong coercivity enhancement where one would expect no such effect. This enhancement is related to the AF susceptibility and is due to an increase in anisotropy. We advance the explanation that spin fluctuations in the AF layer above T_N induce an additional anisotropy in the F layer, an idea supported by a treatment of the total free energy of the bilayer.

II. EXPERIMENTAL CONSIDERATIONS

Single-crystal thin-film AFs are deposited on single-crystal fluoride substrates as in Fig. 1. A bulk single crystal of FeF_2 was oriented with the (110) planes parallel to a surface and mechanically polished. The crystal was then transferred to a high-vacuum electron-beam evaporation system with a base pressure in the 10^{-8} Torr range. The surface of the crystal was then cleaned by repeated annealing to 500 C *in vacuo* before deposition of $\text{ZnF}_2[110]/\text{FeF}_2[110]/\text{Fe}(\text{poly})/\text{Al}(\text{cap})$. The deposition temperatures are identical to previous publications¹³⁻¹⁵ (200, 200, 150, and 150 C, respectively), while the deposition rates were 2 \AA s^{-1} for the fluorides and $<1 \text{ \AA s}^{-1}$ for the metallic layers. X-ray diffraction with the scattering vector out of, and in, the sample plane proved that the fluoride layers were in fact single crystalline, while the Fe overlayers were polycrystalline with

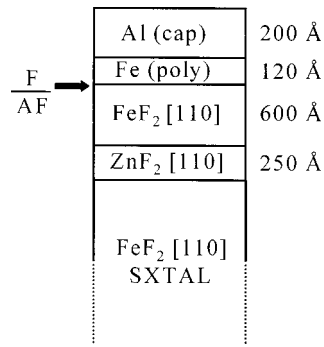


FIG. 1. Schematic of the sample structure.

[110] texturing. The measurements consist of conventional superconducting quantum interference device (SQUID) magnetometry and ferromagnetic resonance (FMR). The FMR measurements were made with the sample oriented film side down on the bottom of a TE 104 mode rectangular cavity, placed between the pole pieces of an electromagnet. The system is operated at 35 GHz and has a loaded Q of approximately 1500.

III. RESULTS

Figures 2(a)–2(c) summarize the magnetometry measurements. Figure 2(a) shows the dependence of the susceptibility (χ) of the AF bulk single crystal. It must be stressed that this is the susceptibility of the bulk crystal and not the AF thin film, which is well below the sensitivity limit of the SQUID. However, given that the AF thin film is grown epitaxially on the crystal, and that the Néel temperature of the film is observed to be identical to that of the bulk crystal it is reasonable to assume that their magnetic properties are similar. (We deduce that the film and bulk Néel temperatures are the same from the fact that the exchange bias in these AF/F bilayers disappears at a blocking temperature which is virtually identical to the bulk Néel temperature.) The $\chi(T)$ behavior is typical of a single-crystal AF.¹⁹ With the field oriented parallel to the easy axis of the AF (i.e., [001]) the susceptibility shows a cusp at T_N and $\chi \rightarrow 0$ as $T \rightarrow 0$. With the field perpendicular to the AF easy anisotropy axis (i.e., [1-1 0]) χ remains finite at low temperatures.

The data of Figs. 2(b) and 2(c) show that the perpendicular coupling mechanism known to exist in this compensated AF system¹⁴ dominates the magnetic response. This behavior is the subject of a separate publication, which probes the magnetic structure with polarized neutron reflectometry.¹⁸ Although we will leave a full discussion of this effect to a separate publication, we explain here how the perpendicular coupling gives rise to the behavior shown. At 300 K, the easy axis of the ferromagnet is the [001] direction, while the [1-1 0] is a hard direction. This is deduced from the fact that the [001] direction has a high coercivity and high “squareness ratio” (M_R/M_S —the ratio of remnant magnetization to saturation magnetization), while the [1-1 0] has low coercivity and squareness. However, on cooling below T_N , the values of M_R/M_S and H_C suggest that the easy and hard axes have swapped such that [001] is now the hard direction and

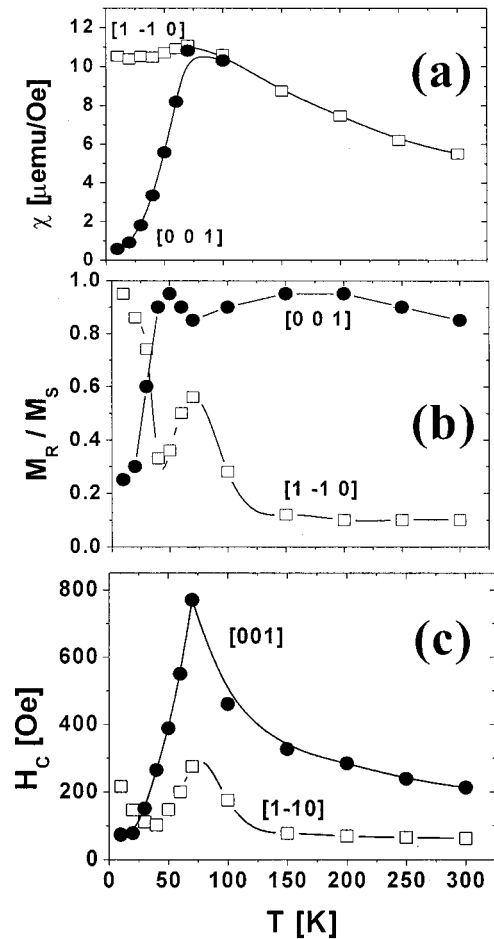


FIG. 2. Summary of the magnetometry measurements as a function of temperature, with the field parallel to [001] (closed symbols) and [1-10] (open symbols). The data were taken after field cooling to 5 K in a field of 2 k Oe. (a) Shows the susceptibility of the AF bulk single crystal, $\chi(T)$; (b) Shows the squareness ratio, $M_R/M_S(T)$; and (c) Shows the coercivity, $H_C(T)$. For FeF_2 , $T_N = 78$ K. The lines are guides to the eye.

[1-1 0] is the easy direction. In other words, the easy axis of magnetization has rotated by 90° on cooling. This would appear to be a clear indication of perpendicular coupling between the AF and F layers and has been observed before in bulk single crystals.¹⁴

The intriguing aspect of the data shown in Fig. 2(c) that is *not* explained by the perpendicular coupling, is the fact that H_C is strongly enhanced *above* T_N . Although relatively small increases in H_C have been observed in the vicinity of T_N or just above it,^{7,10,13–15,20,21} this is a far more dramatic effect. Note that the enhancement persists to well over 300 K, i.e., $>4T_N$, and that ZnF_2/Fe bilayers, which are structurally very similar but have no AF layer, show no such coercivity increase.⁷

The unexpected increase in H_C (above T_N) is further examined in Fig. 3, where the T dependence of the AF susceptibility and the F coercivity are compared.²² The T dependence of the AF susceptibility and the F coercivity are intriguingly similar. This is illustrated more meaningfully on the right-hand panels where $\chi^{-1}(T)$ and $H_C^{-1}(T)$ are plotted. As expected, the susceptibility shows a Curie–Weiss-type

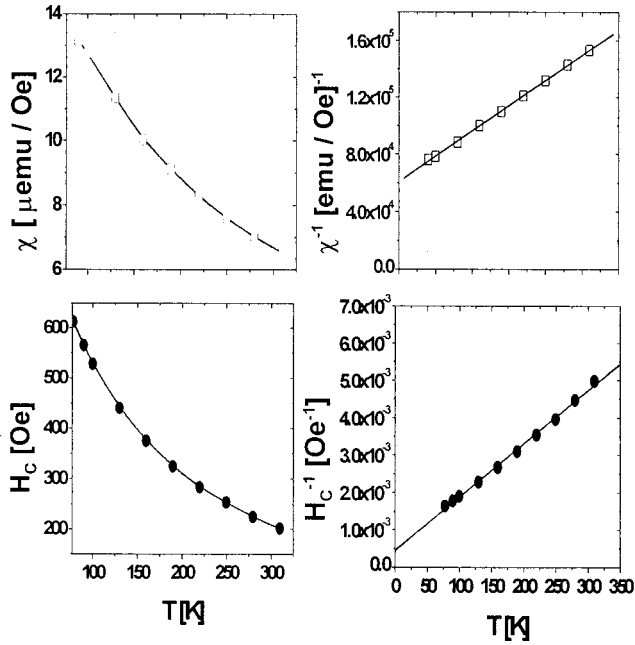


FIG. 3. Comparison of the temperature dependence of the AF susceptibility (χ) and the F coercivity (H_C) for field along [001]. The left panels show $\chi(T)$ and $H_C(T)$ (solid lines are guides to the eye), while the right panel show $\chi^{-1}(T)$ and $H_C^{-1}(T)$ (solid lines are Curie-Weiss law fits).

behavior, $\chi = A/(T + \theta)$ (A is a constant) with a temperature intercept of approximately $\theta = -125$ K. This gives a value for θ/T_N of 1.6 which is in good agreement with previous measurements.¹⁹ Remarkably, H_C follows a similar $H_C \approx B/(T + C)$ behavior (B and C are constants), showing that the F layer coercivity is strongly correlated with the AF susceptibility.

The angular dependence of the H_C enhancement above T_N is displayed in Fig. 4, which shows a polar plot of the

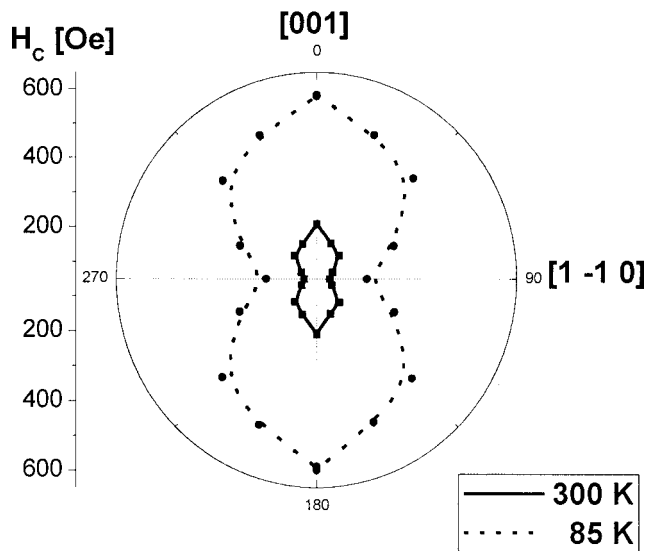


FIG. 4. Polar plot of the in-plane angular dependence of the F layer coercivity, H_C , at 300 and 85 K. The [001] direction is defined as $\theta = 0^\circ$. The squares correspond to 300 K, while the circles are at 85 K. The lines are guides to the eye.

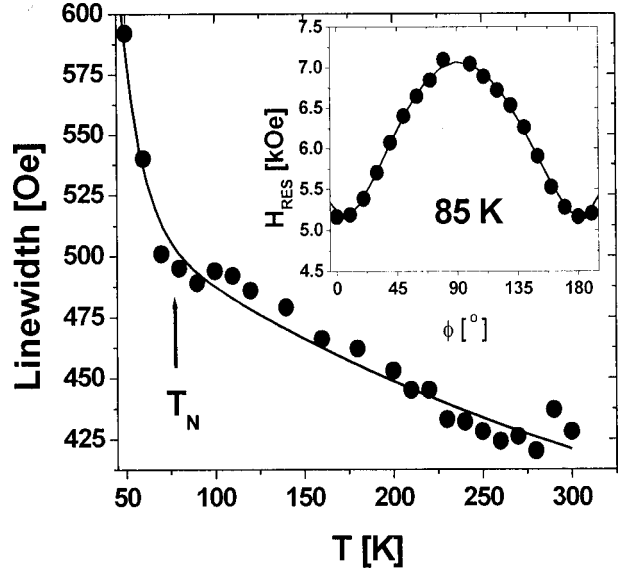


FIG. 5. Temperature dependence of the FMR linewidth, Γ , from 50 to 300 K. The solid line is a guide to the eye. T_N is labeled. Inset: Angular dependence of the FMR resonance field H_{res} at 85 K. The solid line is sinusoidal fit.

coercivity as a function of in-plane angle. As already discussed, the [001] is the easy direction at 300 K, while the [1-1 0] is a hard axis. The data take the shape of a “peanut” which is seen to expand as T is lowered to 85 K and the coercivities increase. We should comment at this stage that this strong enhancement in H_C is unlikely to be driven by magnetoelastic effects as the lattice parameter ratio (c/a) for the body-centered tetragonal FeF_2 only changes by a factor of 1.0006 on cooling from 300 to 100 K.¹⁴

The magnetic anisotropy was also probed by FMR as shown in the inset of Fig. 5. FMR was used as a direct measure of the anisotropy, independent of the complex behavior of the coercivity in this system. The $H_{res}(\theta)$ at 85 K clearly shows a large uniaxial anisotropy in agreement with data of Fig. 4. Note that no unidirectional anisotropy was observed, as expected when $T > T_N$. Fitting to the FMR data assuming a simple uniaxial anisotropy gives $K_2 = 9.5 \times 10^5$ erg/cm³, a clear increase over the room-temperature value of 5.5×10^5 erg/cm³, extracted in a similar fashion. Hence, the H_C enhancement above T_N is not only intimately related with the AF susceptibility but is also driven by an increase in uniaxial magnetic anisotropy. The T dependence of the FMR linewidth (Γ) was also investigated in the temperature range of interest, as shown in Fig. 5. There is a sharp increase in Γ as the bilayer is cooled through T_N which is unsurprising. The most striking feature of the data though is the monotonic increase with reducing T even above T_N . A direct interpretation is that even at temperatures above the Néel point the resonance properties of the F layer are being affected in some manner by the AF beneath. Clearly this is an interesting observation in terms of the H_C enhancement we observe above T_N . It is worth noting at this point that although the coercivity and the linewidth both probe the F layer, and both show anomalous increases, they probe on very different time scales. The FMR probes in the gigahertz regime while the

magnetometry measurements are made over time periods of the order of many minutes.

IV. DISCUSSION AND THEORETICAL TREATMENT

The explanation we wish to advance for the observed phenomenon is simple. We propose that the H_C enhancement is due to the effects of the surface antiferromagnetic spin fluctuations, which are known to exist in AF systems as T_N is approached from above. These fluctuations, which exist on short length and time scales, are the precursors of the full AF ordering, which occurs at T_N . Such short-range ordering behavior has been investigated in the past (even in fluorides^{23,24}) by methods such as neutron diffraction,^{25,26} muon spin rotation,^{24,25} and Mössbauer effect,²⁵ all of which probe short time scale spin structures. It is important to note that with these techniques, it is possible to observe the fluctuations up to temperatures $\sim 10T_N$.²⁵ The spin fluctuations are obviously intimately linked to the antiferromagnetic susceptibility, which grows as the fluctuations increase in spatial and temporal extent. This naturally explains the observed correlation between H_C and χ , and is also consistent with the observed increase in FMR linewidth. Our model also naturally explains why the coercivity enhancement persists to such high temperatures—the fluctuations actually exist up to many times T_N .^{23–26}

We can conceive of at least two precise mechanisms which could give rise to the H_C enhancement. First of all, the proximity of the AF surface to the ordered F layer could “harden” the spin fluctuations into short-range ordered AF regions which are static on the length scale of the field sweeps used to measure H_C . These AF clusters would play the role of the perpendicular domains, which have been suggested as a simple explanation for coercivity enhancements.^{4,5,7} In essence, the AF clusters provide effective pinning centers when a domain wall is swept through the F layer, increasing H_C . The problem with such a picture is that we have conclusively shown that the increase in H_C is correlated with an increase in *anisotropy*. This mechanism creates a coercivity enhancement simply by pinning of domain walls rather than by increases in anisotropy. It should also be noted that similar polycrystalline Fe films on FeF₂ have been proven to have a magnetization reversal at $T > T_N$ which occurs (at least in part) by rotation rather than by domain wall motion.¹⁸ As a final comment on this scenario, we would like to point out that although it creates a H_C enhancement the bias is expected to be zero above T_N as the coupling between the F layer and the total number of clusters averages (spatially) to zero.

A second possible situation is that the spin fluctuations in the AF generate an extra anisotropy in the F layer via an interaction between the two. We mean by this that there is an induced interfacial anisotropy which exists in the interfacial layers of the ferromagnet. This explains all of the data including the observed increase in anisotropy. It is this mechanism which we will now illustrate with a quantitative treatment.

We may write the total free energy of the AF/F system as

$$e^{-\beta F} = \int \Pi dM_F \Pi dM_{AF} e^{-\beta(H_F + J_{AF} + H_{INT})}, \quad (1)$$

where $\beta = 1/kT$ and H_F , H_{AF} , and H_{INT} are the total energies of the F film, AF film, and the coupling energy between them. The integrations are performed over the magnetizing fields and the $\Pi_i dM_i$'s are the respective volume elements. Since $T_C \gg T_N$, the integration over M_F may be dropped, the saturation value being used for M_F wherever it occurs. The integration is thus restricted to the AF degrees of freedom alone. In other words, $F = H_F + F'$, where the partial free energy F' is found from

$$e^{-\beta F'} = \int \Pi dM_{AF} e^{-\beta(H_{AF} + H_{INT})}. \quad (2)$$

We eventually write this integral as an average of $\langle e^{-\beta H_{INT}} \rangle$ of this expression over M_{AF} distributed according to $e^{-\beta H_{AF}}$. We adopt the simplest Ginzburg-Landau model that will allow for AF ordering along an easy anisotropy direction. We denote by \bar{M}_A, \bar{M}_B , the magnetization on the lattice sites of types A and B of the AF and write

$$H_{AF} = \frac{1}{2} \sum_{i=1}^3 g_i [(M_A^i)^2 + (M_B^i)^2] + \frac{g_1 T_N}{T} (\bar{M}_A \cdot \bar{M}_B) + \frac{1}{2} k (\bar{M}_A \cdot \bar{M}_B)^2. \quad (3)$$

Here, the g_i are the three anisotropy energies in the three directions of a simple cubic lattice, with $0 < g_1 < g_2 \leq g_3$, and k is a positive constant. The equations for the minimum H_{AF} , which determine the most probable magnetizations are

$$g_i M_A^i + \frac{g_1 T_N}{T} M_B^i + k (\bar{M}_A \cdot \bar{M}_B) M_B^i = 0, \quad (4)$$

$$g_i M_B^i + \frac{g_1 T_N}{T} M_A^i + k (\bar{M}_A \cdot \bar{M}_B) M_A^i = 0.$$

These have a solution with $M_B^1 = -M_A^1$ and the other two M components equal to zero, provided $T < T_N$. All three components are zero for $T > T_N$ as required. The hierarchy of g 's has been chosen so that the transition favors alignment along the x axis.

To evaluate F' , we use the cumulant theorem for the thermodynamic average

$$\langle e^{-\beta H_{INT}} \rangle = \exp(\langle e^{-\beta H_{INT}} \rangle_{\text{cum}} - 1), \quad (5)$$

in terms of which

$$e^{-\beta F'} = \langle e^{-\beta H_{INT}} \rangle \int \Pi dM_{AF} e^{-\beta H_{AF}}. \quad (6)$$

Above T_N , the bilinear approximation to H_{AF} is sufficient, and \bar{M}_A and \bar{M}_B may be replaced by \bar{M}_A and $-\bar{M}_A$ with all components having zero mean value. The coupling energy is taken in the form

$$H_{INT} = J_{INT} \bar{M}_F \cdot \bar{M}_{AF} \quad (7)$$

and is restricted to the immediate vicinity of the interface only. If $J_{INT} \ll kT$,²⁷ the second-order cumulant moment of βH_{INT} should suffice, so that

$$\langle e^{-\beta H_{INT}} \rangle \approx \beta^2 \langle H_{INT}^2 \rangle \quad (8)$$

and we have

$$\langle \beta^2 H_{\text{INT}}^2 \rangle = J_{\text{INT}}^2 \beta \sum_{i,j} \bar{M}_F^i \bar{M}_F^j \chi_{ij} \quad (9)$$

where,

$$\chi_{ij} = \beta N \int e^{-\beta H_{\text{AF}}} \bar{M}_{\text{AF}}^i \bar{M}_{\text{AF}}^j \Pi \, dM_{\text{AF}} \quad (10)$$

with $N = (\int e^{-\beta H_{\text{AF}}} \Pi \, dM_{\text{AF}})^{-1}$. But these are just the components of the AF susceptibility tensor, i.e., they are the surface magnetization components in the i direction produced in the AF by a small surface-confined magnetic field in the j direction. Keeping only the bilinear terms in H_{AF} [Eq. (2)], and setting $M_A = -M_B = M_{\text{AF}}$ results in a diagonal tensor with elements

$$\chi_{11} = \frac{1}{2g_1(1-T_N/T)}, \quad \chi_{22} = \frac{1}{2g_2}, \quad \chi_{33} = \frac{1}{2g_3} \quad (11)$$

in the vicinity of $T > T_N$. For arbitrarily large values of T the Gaussian approximation fails, because it does not respect the maximum-allowed value of M . If that maximum is taken into account, all the χ 's eventually decrease as T^{-1} . In any case, Eq. (9) indicates that *anisotropy (and therefore a coercive field) has been induced in the interfacial region of the F layer*. Note that the easy axis, and therefore the largest coercivity, occurs along the ordering direction of the antiferromagnet (i.e., its easy direction), just as observed. The effective F energy is now

$$H_F - \frac{1}{\beta} \ln F' = H_F - J_{\text{INT}} \sum_{i=1}^3 \chi_i (M_F^i)^2. \quad (12)$$

Strictly speaking, the susceptibilities described here are surface susceptibilities, and while they may be expected to agree more or less with the shape of the bulk susceptibilities, their magnitudes differ. Suffice to say that there should be a strong correlation between the coercivity enhancement (due to the induced anisotropy) and the bulk susceptibility. It is worth noting that exchange bias and coercivity have been used as a probe of AF surface magnetic properties in the past.²⁸ Again, we should make clear that this model leads to a H_C enhancement above T_N (via the increased uniaxial anisotropy) but not to exchange bias, as no unidirectional anisotropy is induced in the F layer.

Finally, it is worthwhile commenting on the fact that this coercivity enhancement above T_N has not been clearly observed in the past in polycrystalline thin films or twinned epitaxial films. This obviously leads us to suggest that single-crystal conditions are required for the effect to be observed. This could well be due to superior interfacial crystalline orientation not found in twinned or polycrystalline thin films. However, it is worth mentioning that measurements on twinned FeF_2/Fe samples have indicated a small increase in coercivity above T_N , of the order of 100 Oe.²⁹ This could well be the remnant of the effect we see in this paper, diminished by the increased disorder.

V. SUMMARY AND CONCLUSIONS

In summary, we have deposited AF/F bilayers with single-crystal AF thin films by depositing on single-crystal fluoride substrates. An unexpected coercivity enhancement was observed *above* T_N , which was correlated with the AF susceptibility, the FMR linewidth, and the increase of a two-fold uniaxial anisotropy in the F layer. We have interpreted such an effect in terms of AF spin fluctuations at the surface of the AF layer inducing a uniaxial anisotropy in the interfacial region of the F layer which leads to a coercivity enhancement. This scenario was illustrated with the aid of a quantitative treatment of the situation via a thermodynamical calculation.

ACKNOWLEDGMENTS

We thank K. Liu, M. Fitzsimmons, A. Hoffmann, and J. Sivertsen for illuminating discussions. This work was supported by the U.S. DOE (Miami and UCSD), NSF (UCSD), and the UMN Office of Vice President for Research. J. N. acknowledges assistance from Catalan DGR (1999SGR00340).

- ¹Review J. Nogués and I. K. Schuller, *J. Magn. Magn. Mater.* **192**, 203 (1999).
- ²W. H. Meiklejohn and C. P. Bean, *Phys. Rev.* **102**, 1413 (1956).
- ³B. Dieny, V. S. Speriosu, S. S. P. Parkin, B. A. Gurney, D. R. Wilhoit, and D. Mauri, *Phys. Rev. B* **43**, 1297 (1997).
- ⁴D. V. Dimitrov, S. Zhang, J. Q. Xiao, G. C. Hadjipanayis, and C. Prados, *Phys. Rev. B* **58**, 12 090 (1998).
- ⁵S. Zhang, D. V. Dimitrov, G. C. Hadjipanayis, J. W. Cai, and C. L. Chien, *J. Magn. Magn. Mater.* **198–199**, 468 (1999); Z. Li and S. Zhang, *Phys. Rev. B* **61**, R14 897 (2000).
- ⁶T. C. Schulthess and W. H. Butler, *Phys. Rev. Lett.* **81**, 4516 (1998).
- ⁷C. Leighton, J. Nogués, B. J. Jönsson-Åkerman, and I. K. Schuller, *Phys. Rev. Lett.* **84**, 3466 (2000).
- ⁸A. P. Malozemoff, *J. Appl. Phys.* **63**, 3874 (1988).
- ⁹Y. J. Tang, B. Roos, T. Mewes, S. O. Demokritov, B. Hillebrands, and Y. J. Wang, *Appl. Phys. Lett.* **75**, 707 (1999).
- ¹⁰M. D. Stiles and R. D. McMichael, *Phys. Rev. B* **63**, 064405 (2001).
- ¹¹T. Ambrose, R. L. Sommer, and C. L. Chien, *Phys. Rev. B* **56**, 83 (1997); X. W. Wu and C. L. Chien, *Phys. Rev. Lett.* **81**, 2795 (1998); N. J. Göke-meijer and C. L. Chien, *J. Appl. Phys.* **85**, 5516 (1999); T. Ambrose and C. L. Chien *ibid.* **83**, 6822 (1998).
- ¹²V. I. Nikitenko, V. S. Gornakov, A. J. Shapiro R. D. Shull, K. Liu, S. M. Zhou, and C. L. Chien, *Phys. Rev. Lett.* **84**, 765 (2000).
- ¹³M. R. Fitzsimmons, P. Yashar, C. Leighton, I. K. Schuller, J. Nogués, C. F. Majkrzak, and J. A. Dura *Phys. Rev. Lett.* **84**, 3986 (2000); C. Leighton, M. R. Fitzsimmons, P. Yashar, A. Hoffmann, J. Nogués, J. Dura, C. F. Majkrzak, and I. K. Schuller, *ibid.* **86**, 4394 (2001).
- ¹⁴T. J. Moran, J. Nogués, D. Lederman, and I. K. Schuller, *Appl. Phys. Lett.* **72**, 617 (1998).
- ¹⁵J. Nogués, D. Lederman, T. J. Moran, I. K. Schuller, and K. V. Rao, *Appl. Phys. Lett.* **68**, 3186 (1996).
- ¹⁶N. C. Koon, *Phys. Rev. Lett.* **78**, 4865 (1997).
- ¹⁷Y. Ijiri, J. A. Borchers, R. W. Erwin, S.-H. Lee, P. J. van der Zaag, and R. M. Wolf, *Phys. Rev. Lett.* **80**, 608 (1998).
- ¹⁸M. R. Fitzsimmons, C. Leighton, J. Nogués, A. Hoffmann, I. K. Schuller, K. Liu, C. F. Majkrzak, J. A. Dura, J. R. Groves, R. W. Springer, P. N. Arendt, V. Leiner, and H. Lauter (unpublished).
- ¹⁹C. Kittel, *Introduction to Solid State Physics*, 6th ed. (Wiley, New York, 1991) p. 445.
- ²⁰F. B. Hagedorn, *J. Appl. Phys.* **38**, 3641 (1967).
- ²¹S. H. Charap and E. Fulcomer, *J. Appl. Phys.* **42**, 1426 (1971).
- ²²Note that the data of Fig. 3 were taken in a separate temperature sweep than that of Fig. 2(c), with more closely spaced points. The slight difference in maximum coercivity is due to small and unavoidable irreproduc-

ibilities due to misalignment of the single crystal with the magnetic field. This is a consequence of the small size of the single crystal.

- ²³M. G. Cottam, V. So, D. J. Lockwood, R. S. Katiyar, and H. J. Guggenheim, *J. Phys. C* **16**, 1741 (1983).
- ²⁴S. R. Brown, M. Attenborough, I. Hall, O. Nikolov, and S. F. J. Cox, *Philos. Mag. Lett.* **73**, 195 (1996); M. Attenborough, I. Hall, O. Nikolov, S. R. Brown, and S. F. J. Cox, *Hyperfine Interact.* **108**, 423 (1997).
- ²⁵W. Potzel, G. M. Kalvius, W. Schiessl, H. Karzel, M. Steiner, A. Kratzer, A. Martin, M. K. Krause, A. Sneider, I. Halevy, J. Gal, W. Schafer, G. Will, M. Hillberg, R. Wappling, D. W. Mitchell, and T. P. Das, *Hyperfine Interact.* **97**, 373 (1996).
- ²⁶I. A. Blech and B. L. Averbach, *Physics (Long Island City, N.Y.)* **1**, 31 (1964).
- ²⁷This is a reasonable approximation as the exchange field of this system is 50 Oe at most.
- ²⁸D. Lederman, J. Nogués, and I. K. Schuller, *Phys. Rev. B* **56**, 2332 (1997).
- ²⁹P. Miltényi, M. Gruyters, G. Güntherodt, J. Nogués, and I. K. Schuller (unpublished).